More About This Article

Additional resources and features associated with this article are available within the HTML version:

- Supporting Information
- Links to the 3 articles that cite this article, as of the time of this article download
- Access to high resolution figures
- Links to articles and content related to this article
- Copyright permission to reproduce figures and/or text from this article

View the Full Text HTML

New Insights into α-GalNAc−Ser Motif: Influence of Hydrogen Bonding versus Solvent Interactions on the Preferred Conformation

Francisco Corzana,[†] Jesús H. Busto,[†] Gonzalo Jiménez-Osés,[†] Juan L. Asensio,[‡] Jesús Jiménez-Barbero,[§] Jesús M. Peregrina,*,[†] and Alberto Avenoza*,[†]

Contribution from the Departamento de Química, Universidad de La Rioja, UA-CSIC, Madre de Dios 51, E−26006 Logroño, Spain, Instituto de Química Orgánica General, CSIC, Juan de la Cierva 3, E−28006 Madrid, Spain, and Departamento de Estructura y Función de Proteínas, Centro de Investigaciones Biológicas, CSIC, Ramiro de Maeztu 9, E−28040 Madrid, Spain

Received July 7, 2006; E-mail: alberto.avenoza@dq.unirioja.es

Abstract: The structural features of the mucin-type simplest model, namely, the glycopeptide α-*O*-GalNAc-L-Ser diamide, have been investigated by combining NMR spectroscopy, molecular dynamics simulations, and DFT calculations. In contrast to previous reports, the study reveals that intramolecular hydrogen bonds between sugar and peptide residues are very weak and, as a consequence, not strong enough to maintain the well-defined conformation of this type of molecule. In fact, the observed conformation of this model glycopeptide can be satisfactorily explained by the presence of water pockets/bridges between the sugar and the peptide moieties. Additionally, DFT calculations reveal that not only the bridging water molecules but also the surrounding water molecules in the first hydration shell are essential to keep the existing conformation.

Introduction

The α-*O*-glycosidic linkage between *N*-acetylated 2-amino-2-deoxy-D-galactose (GalNAc) and the hydroxyl group of L-serine (Ser) or L-threonine (Thr) has attracted much attention in recent years,[1] from many different viewpoints. In fact, this is a common pattern in numerous glycoproteins (i.e. mucins[2]), which are involved in fundamental biological processes[3] such as inflammation, inmune response, cell−cell communication, cell growth, cell adhesion, and antifreeze activity, among others. Moreover, mucins are attracting real interest in therapeutic approaches,[4] specially for the development of vaccines for cancer treatment.[5]

On the other hand, it has been described that in Nature, α-*O*-glycosylation has a profound organizational effect on the underlying peptide backbone, forcing it into an extended conformation.[1b,6] Several attempts have tried to find an explana-tion for this fact, since to discern how glycoproteins interact with their biological targets it is essential to improve our understanding of the mechanisms that allow the carbohydrate to modify the conformational equilibrium of the peptide backbone. At the present moment, the conformational bias observed upon α-*O*-glycosylation is explained by means of specific hydrogen bonds between the peptide moiety and the first GalNAc unit, which "lock" the orientation of the sugar with respect to the peptide backbone.[1b,c,7]

However, opposite to this currently used thesis, we demonstrate herein that this interaction is not responsible for the extended conformation of the backbone. To reach this conclusion, we have carried out the synthesis and structural study of the simplest model glycopeptide α-*O*-GalNAc-L-Ser diamide **1**, at natural abundance and also isotopically labeled with [15]N (10%) and [13]C (100%) at key positions (Figure 1). A careful

---

† Universidad de La Rioja.
‡ Instituto de Química Orgánica General, CSIC.
§ Centro de Investigaciones Biológicas, CSIC.

(1) (a) Live, D. H.; Williams, L. J.; Kuduk, S. D.; Schwarz, J. B.; Glunz, P. W.; Chen, X.-T.; Sames, D.; Kumar, R. A.; Danishefsky, S. J. *Proc. Natl. Acad. Sci. U.S.A.* **1999**, *96*, 3489−3493. (b) Coltart, D. M.; Royyuru, A. K.; Williams, L. J.; Glunz, P. W.; Sames, D.; Kuduk, S.; Schwarz, J.; Chen, X.-T.; Danishefsky, S. J. *J. Am. Chem. Soc.* **2002**, *124*, 9833−9844. (c) Csonka, G. I.; Schubert, G. A.; Perczel, A.; Sosa, C. P.; Csizmadia, I. G. *Chem.−Eur. J.* **2002**, *8*, 4718−4733. (d) Tachibana, Y.; Fletcher, G. L.; Fujitani, N.; Tsuda, S.; Monde, K.; Nishimura, S.-I. *Angew. Chem., Int. Ed.* **2004**, *43*, 856−862.
(2) (a) Strous, G. J.; Dekker, J. *Crit. Rev. Biochem. Mol. Biol.* **1992**, *27*, 57−92. (b) Hang, H. C.; Bertozzi, C. R. *Bioorg. Med. Chem.* **2005**, *13*, 5021−5034.
(3) (a) Dwek, R. A. *Chem. Rev.* **1996**, *96*, 683−720. (b) Sears, P.; Wong, C.-H. *Cell. Mol. Life Sci.* **1998**, *54*, 223−252.

(4) (a) Davis, B. G. *Chem. Rev.* **2002**, *102*, 579−601. (b) Watt, G. M.; Lund, J.; Levens, M.; Kolli, V. S. K.; Jefferis, R.; Boons, G.-J. *Chem. Biol.* **2003**, *10*, 807−814. (c) Lui, H.; Wang, L.; Brock, A.; Wong, C.-H.; Schultz, P. G. *J. Am. Chem. Soc.* **2003**, *125*, 1702−1703. (d) Gamblin, D. P.; Garnier, P.; van Kasteren, S.; Oldham, N. J.; Fairbanks, A. J.; Davis, B. G. *Angew. Chem., Int. Ed.* **2004**, *116*, 827−833. (e) Davis, B. G. *Science* **2004**, *303*, 480−482.
(5) (a) Dube, D. H.; Prescher, J. A.; Quang, C. N.; Bertozzi, C. R. *Proc. Natl. Acad. Sci. U.S.A.* **2006**, *103*, 4819−4824. (b) Hill, C. A. S.; Bullard, K. A.; Walcheck, B. *Cancer Lett.* **2005**, *217*, 105. (c) Jaracz, S.; Chen, J.; Kuznetsova, L. V.; Ojima, I *Bioorg. Med. Chem.* **2005**, *13*, 5043−5054. (d) Danishefsky, S. J.; Allen, J. R. *Angew. Chem., Int. Ed.* **2000**, *39*, 836−863.
(6) Pratt, M. R.; Bertozzi, C. R. *Chem. Soc. Rev.* **2005**, *34*, 58−68.
(7) (a) Mimura, Y.; Inoue, Y.; Maeji, N. J.; Chûjô, R. *Int. J. Pept. Protein Res.* **1989**, *34*, 363−368. (b) Shuman, J.; Qiu, D.; Koganty, R. R.; Longenecker, B. M.; Campbell, A. P. *Glycoconjugate J.* **2000**, *17*, 835−848. (c) Tachibana, Y.; Monde, K.; Nishimura, S.-I. *Macromolecules* **2004**, *37*, 6771−6779.
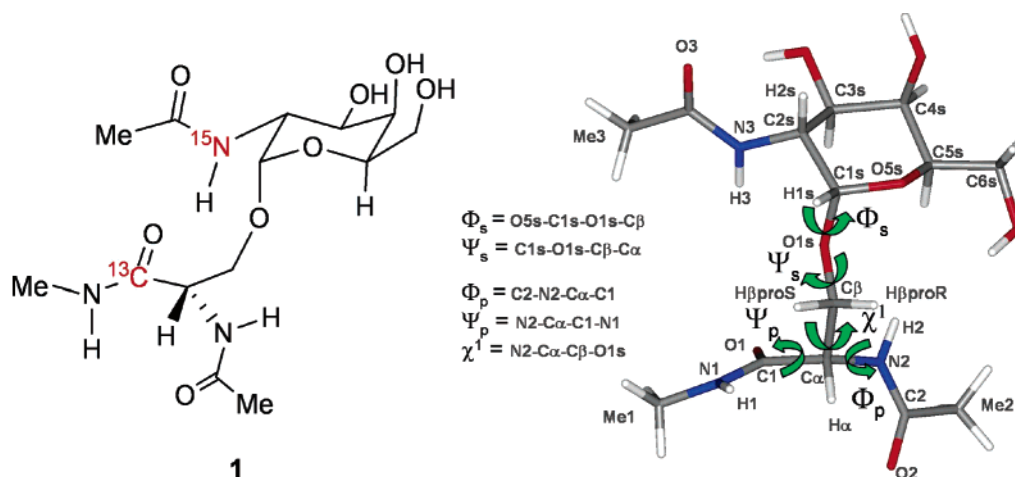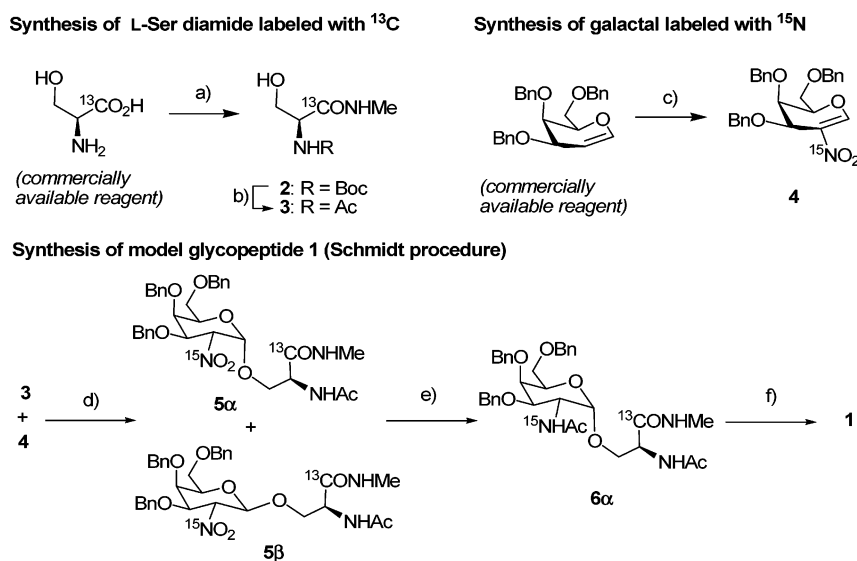
Figure 1. Representative 2D- and 3D-structures of model glycopeptide **1**, including atomic and dihedral labels employed in this work.

Scheme 1. Synthetic Route to **1**[a]

[a] (a) (i) Boc₂O, 1 N aq NaOH, dioxane, rt, 24 h, (ii) MeNH₂·HCl, TBTU, DIEA, MeCN, rt, 10 h, 64%; (b) (i) TFA, CH₂Cl₂, rt, 3.5 h, (ii) Ac₂O, Py, rt, 3 h, (iii) MeONa, MeOH, rt, 3 h, 73%; (c) (i) concd aq H¹⁵NO₃, Ac₂O, −50 °C, 0.5 h, (ii) Et₃N, CH₂Cl₂, rt, 0.5 h, 81%; (d) ᵗBuOK, THF, rt, 12 h, 60%; (e) (i) Raney nickel T4 (Pt), H₂, EtOH, 1 atm, rt, 3 h, (ii) Ac₂O, Py, rt, 3 h, (iii) separation by column chromatography, 83%; (f) H₂, Pd/C, MeOH−EtOAc, 1 atm, rt, 12 h, 100%.

conformational analysis of **1** has been carried out using NMR (NOE and homo- and heteronuclear coupling constants, using the labeled molecule), which have been interpreted with the assistance of molecular dynamics (MD) simulations. No experimental evidence of direct intramolecular hydrogen bond was found between the ¹³C labeled carbonyl group of the serine moiety and the amide proton of GalNAc. This analysis, together with DFT calculations carried out, including explicit water molecules for the first hydration shell, points toward the existence of bridging water molecules between the sugar and the peptide moieties, which could indeed explain the stabilization of the extended conformation of the simulated backbone. Thus, the population of conformers showing the above-mentioned direct intramolecular hydrogen bond must be intrinsically very low.
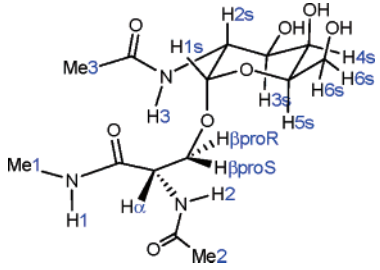
Results

Synthesis. Model glycopeptide **1** was synthesized using the standard Michael-type addition conditions developed by Schmidt and co-workers[8] with L-serine derivative **3** labeled with ¹³C at

the carbonyl group and 3,4,6-tri-*O*-benzyl-2-nitro-D-galactal labeled with ¹⁵N (**4**) (Scheme 1). Thus, the commercially available L-serine labeled with ¹³C was easily transformed into the *N*-Boc derivative following the procedure described in the literature.[9] Then, the treatment of this compound with MeNH₂· HCl and TBTU in the presence of DIEA gave the corresponding methyl amide **2**. Final deprotection of the amino group with TFA, further diacetylation with Ac₂O/Py, and deprotection of the hydroxyl group of serine with MeONa gave the desired compound **3**, with good yield. Nitro-D-galactal **4** was easily obtained following the procedure described in the literature,[8] but employing concentrated HNO₃ labeled with 10% of ¹⁵N in our case. Further treatment of nitro-D-galactal **4** with derivative **3** in the presence of catalytic amounts of ᵗBuOK gave a mixture of two anomers (**5α** and **5β**) in a 9:1 ratio, respectively. The mixture of both anomers was successfully converted into the

(8) (a) Winterfeld, G. A.; Ito, Y.; Ogawa, T.; Schmidt, R. R. *Eur. J. Org. Chem.* **1999**, 1167−1171. (b)Winterfeld, G. A.; Schmidt, R. R. *Angew. Chem., Int. Ed.* **2001**, *40*, 2654−2657.
(9) Campbell, A. D.; Raynham, T. M.; Taylor, R. J. K. *Synthesis* **1998**, 1707−1709.

Table 1. Full Assignment of Protons and $^nJ_{H,H}$ Couplings for **1**[a]

δ (ppm)	proton	splitting[b] (no. of protons)	$^nJ_{H,H}$ (in Hz)
2.05	Me3	s (3H)	—
2.08	Me2	s (3H)	—
2.76	Me1	s (3H)	—
3.72−3.78	H6s[c]	m (2H)	—
3.81	HβproR	dd (1H)	$^2J_{Hβ proR,Hβ proS} = 10.8$
			$^3J_{HβproR,Hα} = 5.5$
3.86−3.94	H3s[c]	m (3H)	—
	HβproS		
	H5s[c]		
3.97−4.00	H4s[c]	m (1H)	—
4.15	H2s[c]	dd (1H)	$^3J_{H2s,H3s} = 11.0$
			$^3J_{H2s,H1s} = 3.7$
4.54	Hα	dd (1H)	$^3J_{Hα,HβproR} = 5.5$
			$^3J_{Hα,HβproS} = 4.5$
4.89	H1s[c]	d (1H)	$^3J_{H1s,H2s} = 3.7$
8.05[d]	N−H3[d]	d (1H)[d]	$^3J_{H3,H2s} = 9.2$[d]
8.05−8.12[d]	N−H1[d]	m (1H)[d]	—
8.42[d]	N−H2[d]	d (1H)[d]	$^3J_{H2,Hα} = 6.2$[d]

[a] Data extracted from 1D ^{1}H NMR experiment carried out in D$_2$O (20 °C, pH = 5.2) at 400 MHz. [b] s = singlet, d = doublet, dd = doublet of doublet, m = multiplet. [c] The letter "s" makes reference to sugar moiety. [d] Data extracted from 1D ^{1}H NMR experiment carried out in H$_2$O/D$_2$O (9/1) (20 °C, pH = 5.2) at 500 MHz.

corresponding amino compounds with Raney nickel T4 (Pt) as a catalyst.[10] The subsequent treatment with Ac$_2$O/Py, further purification of **6α** by column chromatography on silica gel, and deprotection of the hydroxyl groups by hydrogenolysis led to the desired model glycopeptide **1**, in moderate yield (Scheme 1). The glycosylated Ser diamide **1** at natural abundance was synthesized following the same procedure but starting from 3,4,6-tri-*O*-benzyl-2-nitro-D-galactal[8] and Ser diamide as previously described.[11]

NMR Experiments. 1D- and 2D-NOESY Experiments. In a first step, full assignment of protons corresponding to compound **1** was made using COSY and HSQC experiments (see Supporting Information) and it is given in Table 1. Then, selective 1D-NOESY experiments in D$_2$O (20 °C, pH 5.2) and 2D-NOESY experiments in H$_2$O/D$_2$O (9/1) (20 °C, pH 5.2) were carried out for glycopeptide **1** (See Supporting Information and Figure 2). In addition, ^3J coupling constants were measured from the splitting of the resonance signals in the 1D spectrum and are gathered in Table 1.

The strong NOE observed between Hα and H1, together with the weak one between H1 and H2, strongly suggests that the simulated peptide backbone mainly adopts an extended conformation.[12] This is also corroborated when the NOE intensities of the Hα−H2 and Hα−H1 proton pairs are compared. The

first one is much weaker than the second one, in agreement with the expectations for an extended conformation (see Figure 2). On the other hand, NOEs between H1 (amide proton at the Ser methyl acetamide C-terminus) and the GalNAc amide proton (dubbed H3) or its corresponding GalNAc acetamide methyl group (Me3) were not detected, a first suggestion for the lack of importance of hydrogen bonds between the carbohydrate and the peptide moieties (Figure 2).

From a quantitative viewpoint, NOE build up curves were measured (Figure 2c and Supporting Information) and used to extract the corresponding proton−proton distances,[13] which were used for further analysis using MD simulations including experimental restraints.

MD Simulations. Thus, to get an experimentally derived ensemble, 80-ns MD-tar[14] (MD with time-averaged restraints) simulations were carried out by including the coupling constants and distances shown in Table 2 as time-averaged restraints. The simulation was performed without explicit solvent, but using a bulk dielectric constant of 80 to reproduce the water environment.

The calculated ^3J coupling constant values were obtained from the simulations by applying the appropriate Karplus equation[15] to the corresponding torsion angles.

MD-tar simulations were performed with AMBER 6.0[16] (parm94),[17] which was implemented with GLYCAM 04 parameters[18] to accurately simulate the conformational behavior of the sugar moiety. In addition, a 4-ns MD-tar in explicit water, as well as a 40-ns unrestrained MD simulations in explicit water, were also carried out for comparison (MD$_{H2O}$-tar and MD$_{H2O}$ columns, Table 2, respectively).

From inspection of Table 2, it can be deduced that the unrestrained MD simulations (MD$_{H2O}$) fail to accurately reproduce the conformation of the peptide backbone, suggesting a folded conformation (distance H1−H2 < distance Hα-H1) for compound **1**. This result is characteristic of the AMBER94 force field, used in the simulations, which favor helical structures for small peptides.[19] However, when the experimental data was entered as restraints (MD$_{H2O}$-tar and MD-tar), the calculated distances and ^3J values obtained from the MD$_{H2O}$-tar simulations, and in particular from the longer MD-tar simulations, were in good accordance with the experimental values. It is important to point out that when applying restrained MD, the sensitivity of the results to the simulation conditions depends not only on the force field but mainly on the amount of experimental information included as time-averaged constraints. Figure 3 shows the Φ/Ψ distributions of the peptide backbone (Φ$_p$/Ψ$_p$) and the glycosidic linkage (Φ$_s$/Ψ$_s$), as well as the distribution of χ^1, obtained from the MD-tar simulations for glycopeptide

(10) Nishimura, S. *Bull. Chem. Soc. Jpn.* **1959**, *32*, 61−64.
(11) Corzana, F.; Busto, J. H.; Engelsen, S. B.; Jiménez-Barbero, J.; Asensio, J. L.; Peregrina, J. M.; Avenoza, A. *Chem.−Eur. J.* **2006**, *12*, 7664−7771.

(12) Dyson, H. J.; Wright, P. E. *Annu. Rev. Biophys. Chem.* **1991**, *20*, 519−538.
(13) Haselhorst, T.; Weimar, T.; Peters, T. *J. Am. Chem. Soc.* **2001**, *123*, 10705−10714.
(14) Pearlman, D. A. *J. Biomol. NMR* **1994**, *4*, 1−16.
(15) (a) Marco, A.; Llinas, M.; Wuthrich, K. *Biopolymers* **1978**, *17*, 617−636. (b) Vuister, G. W.; Bax, A. *J. Am. Chem. Soc.* **1993**, *115*, 7772−7777.
(16) (a) Pearlman, D. A.; Case, D. A.; Caldwell, J. W.; Ross, W. R.; Cheatham, T. E., III; DeBolt, S.; Ferguson, D.; Seibel, G.; Kollman, P. *Comput. Phys. Commun.* **1995**, *91*, 1−41. (b) Kollman, P. A.; et al. **1999**, AMBER 6, University of California, San Francisco.
(17) Cornell, W. D.; Cieplack, P. C.; Bayly, I.; Gould, I. R.; Merz, K.; Ferguson, D. M.; Spellmeyer, D. C.; Fox, T.; Caldwell, J. W.; Kollman, P. A. *J. Am. Chem. Soc.* **1995**, *117*, 5179−5197.
(18) Woods, R. J.; Dwek, R. A.; Edge, C. J.; Fraser-Reid, B. *J. Phys. Chem. B* **1995**, *99*, 3832−3846.
(19) Gnanakaran, S.; García, A. E. *J. Phys. Chem. B* **2003**, *107*, 12555−12557.
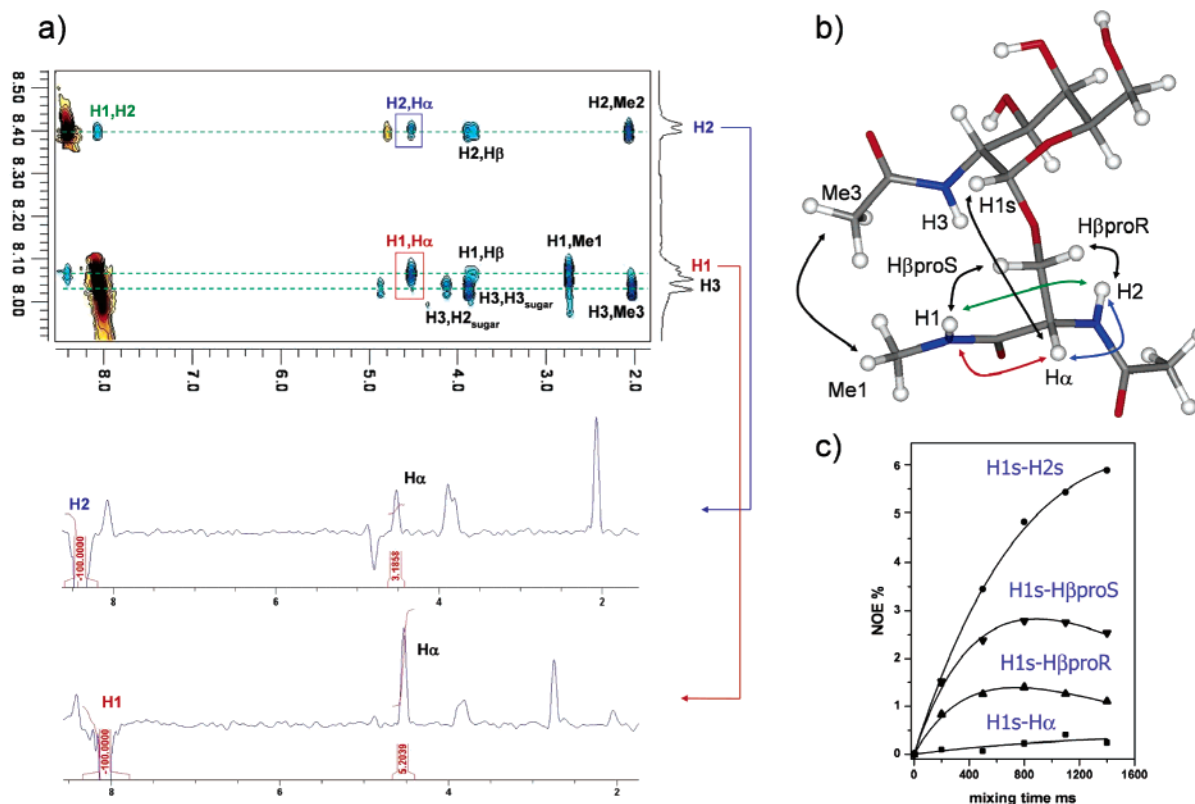
Figure 2. (a) Section of the 800-ms NOESY spectrum (400 MHz) of compound **1** in H_2O/D_2O (9/1) at 20 °C, showing amide−aliphatic cross-peaks. (b) Representative 3D-structure of **1**, showing the most significant NOEs for the conformational analysis. (c) Example of NOE build up curves for H1s of **1**.

Table 2. Comparison of the Experimental and MD Simulations Derived Distances and ^3J Couplings for 1^a

	expl	MD-tar ($\epsilon = 80$)	MD_{H2O}-tar	MD_{H2O}
$d_{H1,H2}$	2.9 (m)^b	2.9	3.2	2.4
$d_{H\alpha,H1}$	2.3 (s)^b	2.5	2.4	3.2
$d_{H\alpha,H2}$	2.9 (m)^b	2.8	2.9	2.9
$d_{H1,H\beta proS}$	2.5	2.3	2.4	2.3
$d_{H1,H\beta proR}$	2.6	2.6	2.6	2.8
$d_{H1s,H\alpha}$	3.9	3.8	3.5	4.5
$^3J_{H\alpha,H\beta pro R}$	5.5	5.8^c	6.4^c	4.1^c
$^3J_{H\alpha,H\beta pro S}$	4.5	4.7^c	4.8^c	3.2^c
$^3J_{H2,H\alpha}$	6.2	6.5^d	6.4^d	6.7^d
$^3J_{H3,H2s}$	9.2	9.3^d	9.4^d	7.9^d

^{a} Distances are given in Å and ^3J coupling in Hz. ^{b} m = medium and s = strong NOE. ^{c} Estimated from the MD simulations using the Karplus equation given in ref 15a. ^{d} Estimated from the MD simulations using the Karplus equation given in ref 15b.

1. It can be observed that according to the NOE experiments commented above, Φ_p/Ψ_p dihedral values (backbone) are similar to those typical for extended conformations, such as PPII and β-sheet, and only a small amount of conformers showed Φ_p/Ψ_p dihedral values corresponding to α-helical structures.

Concerning the glycosidic linkage, Φ_s has a value close to 80°, in accordance with the exo-anomeric effect, while Ψ_s is rather rigid, showing a value about 180°.

The simulations also indicated that χ^1 dihedral showed a conformational preference for values close to 60°. The application of the Karplus equation[15a] for this torsion angle led to theoretical values of $^3J_{H\alpha,H\beta}$ that are in good accordance with the experimentally measured one (Table 2). Besides, this preferred conformation also agrees with the medium observed NOE between the acetamide methyl (Me3) of sugar residue and the methyl amide (Me1) of peptide moiety (see Supporting Information).

As additional indication of the goodness of the obtained conformational distribution, the experimental and theoretical $^3J_{H3,H2s}$ were also in good agreement. This value of ^3J suggests a torsion angle H3−N3−C2s−H2s of about 180°.[15b] Accordingly, the orientation of the *N*-acetyl group relative to the sugar framework seems essentially fixed.

On this basis, we can state that the geometry of the simplest model, glycopeptide **1**, in aqueous solution is essentially equal to that observed in glycopeptides derived from naturally occurring glycoproteins previously studied.[1b,20] Several authors have concluded that the defined geometry of these glycopeptides, in which the peptide backbone adopts an extended conformation, is stabilized by the existence of an intramolecular hydrogen bond between the amide NH proton of GalNAc and the oxygen of the carbonyl group[1b,20a] at the peptide (H3 and O1 in our model compound, respectively). Interestingly, our experimental and theoretical studies (see below) suggest that this hydrogen bond must be very weak.

Experimental Evidences of the Absence of Sugar and Amino Acid Interresidue Hydrogen Bonds. To experimentally estimate the strength of this hydrogen bond[21] and taking into account that the HNCO experiment[21a] failed, 1D-selective HMQC-type experiments were performed on the ^{13}C-labeled

(20) (a) Schuman, J.; Qiu, D. X.; Koganty, R. R.; Longenecker, B. M.; Campbell, A. P. *Glycoconjugate J.* **2000**, *17*, 835−848. (b) Möller, H.; Serttas, N.; Paulsen, H.; Burchell, J. M.; Taylor-Papadimitriou, J.; Meyer, B. *Eur. J. Biochem.* **2002**, *269*, 1444−1455. (c) Kinarsky, L.; Suryanarayanan, G.; Prakash, O.; Paulsen, H.; Clausen, H.; Hanisch, F.-G.; Hollingsworth, M. A.; Sherman, S. *Glycobiology* **2003**, *13*, 929−939.
(21) (a) Barfield, M. *J. Am. Chem. Soc.* **2002**, *124*, 4158−4168. (b) Cordier, F.; Rogowski, M.; Grzesiek, S.; Bax, A. *J. Magn. Reson.* **1999**, *140*, 510−512.
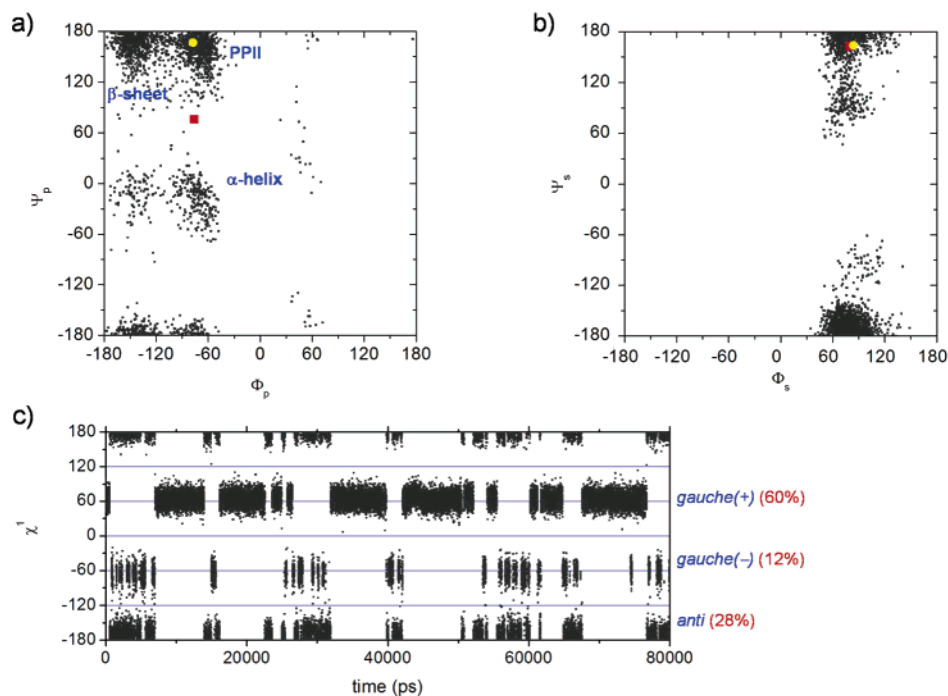
Figure 3. (a) Φ_p/Ψ_p distribution obtained from MD-tar calculations for simulated peptide backbone of **1**. (b) Φ_s/Ψ_s distribution obtained from MD-tar simulations for the glycosidic linkage of **1**. (c) χ^1 distribution obtained from MD-tar simulations of **1**. (Red square) Calculated dihedral angle Φ_p, Ψ_p, Φ_s, and Ψ_s values of the global minimum found for **1** at the HF/6-31G(d) level of theory (ref 1c). (Yellow dot) Dihedral angle Φ_p, Ψ_p, Φ_s, and Ψ_s values of GalNAc−Ser residue found for the average structure of tri-α-STF−STTAV glycopeptide in aqueous solution (ref 1b).

compound **1** in order to determine the $^2J_{C1,H3}$.[21b] Different experiments were performed with the period for evolution of couplings (1/2*J*) chosen to match *J* values of 1, 2, 3, 4, and 5 Hz. No signal for the target H3 proton was observed in any case. Indeed, resonance signals for the Hα and Hβ protons were observed, as well as for the two amide protons located at two or three bonds away from the ^{13}C-labeled carbonyl moiety (H1 and H2, respectively). Moreover, the Me1 protons signal was also observed with high intensity when the *J*-evolution period was matched to 4−5 Hz. When the *J*-evolution period was longer than 200 ms (*J* = 1−2 Hz), the Me2 protons, located at five bonds from the target carbonyl carbon, were also observed. This fact seems to indicate that the persistence of the H3⋯O1 hydrogen bond, if any, must be very low, since no signal for the amide H3 proton was observed at any mixing time.

To shed some light on the factors that govern the experimentally observed shift to extended conformations in the model glycopeptides **1**, we carried out an extensive theoretical study as discussed in the next section.

Solvent Influence on the Conformational Behavior of Compound 1. First, it has to be emphasized that hydrogen bonds between the sugar and the peptide moieties were not detected over the course of the MD simulations. To gain details of the influence of the water on the solute conformation, the number of close neighbor water molecules as a function of time was calculated. The MD$_{H2O}$-tar simulations trajectory was chosen for this purpose because, as commented above, the unrestrained MD simulations did not quantitatively reproduce the experimental data that support the conformational behavior of **1**. The average hydration number was 17.9 and 4.6 for water oxygen distances less than 3.5 and 2.8 Å from the solute heteroatoms (nitrogen and oxygen), respectively. These values are similar to that previously found for a β-*O*-Glc-L-Ser diamide compound.[11] The next stage was to inspect the anisotropic hydration

of the solute. First, the radial pair distribution functions (RDF) were calculated for all heteroatoms of **1**. These RDF functions give the probability, *g*(*r*), of finding a water molecule at a given distance *r* from the solute. Figure 4a shows the RDF obtained from MD$_{H2O}$-tar simulations for atoms O1 and N3. These results are in agreement with previous studies carried out on amides.[22] In addition, normalized two-dimensional radial pair distributions[23] were calculated for all possible shared water density sites (Figure 4b). These 2D functions give the probability, *g*(*r_1*,*r_2*), of finding a water molecule at a distance r_1 and r_2 from two selected solute atoms, relative to the probability expected for a random distribution (Figure 4d). Figure 4b shows the 2D radial pair distribution obtained for atoms N3 and O1. Interestingly, the shared water density found in the first hydration shell (ca. 2.8 Å) of both atoms revealed the existence of bridging water molecules between N3 and O1 (Figure 4c). The density of this shared water site was 1.5 times the bulk density, having maximum and average residence times of 5.5 and 0.5 ps, respectively. The average distance between N3 and O1 was 5.6 Å, ranging from 7.8 to 2.8 Å.

Additionally, different frames of the MD$_{H2O}$-tar simulations containing the first hydration shell and a bridging water molecule were subjected to minimization using DFT methods (Figure 5). From the MD analysis, gauche (−) and gauche (+) conformations of hydroxymethyl group were deduced and considered for these DFT calculations. This study clearly revealed that the

(22) (a) Mennucci, B.; Martínez, J. M. *J. Phys. Chem. B* **2005,** *109,* 9818−9829. (b) Rick, S. W.; Berne, B. J. *J. Am. Chem. Soc.* **1996**, *118*, 672−679. (c) Gao, J.; Freindorf, M. *J. Phys. Chem. A* **1997**, *101*, 3182−3188. (d) Beglov, D.; Roux, B. *J. Phys. Chem. B* **1997**, *101*, 7821−7826. (e) Buck, M.; Karplus, M. *J. Phys. Chem. B* **2001**, *105*, 11000−11015. (f) Rocha, W.; Almeida, K. D.; Coutinho, K.; Canuto, S. *Chem. Phys. Lett.* **2001**, *345*, 171−178. (g) Iuchi, S.; Morita, A.; Kato, S. *J. Phys. Chem. B* **2002**, *106*, 3466−3476.
(23) Andersson, C. A.; Engelsen, S. B. *J. Mol. Graphics Model.* **1999**, *17*, 101−105.
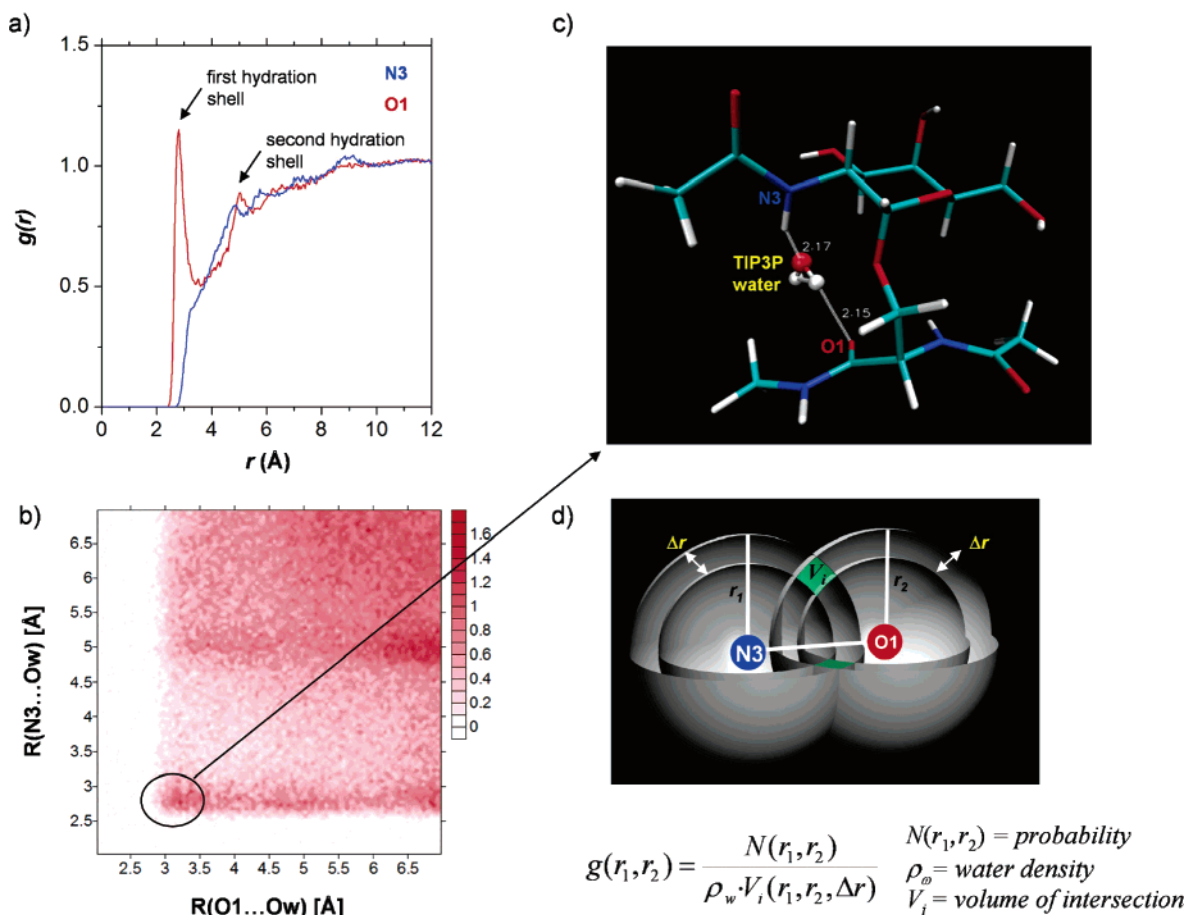
Figure 4. (a) Radial pair distribution function (RDF) of O1 and N3. (b) Two-dimensional radial pair distribution function for O1 and N3 found in the 4-ns MD$_{H2O}$-tar simulation. (c) A representative frame of the 4-ns MD$_{H2O}$-tar simulation showing a bridging water molecule. (d) Schematic diagram of hydration shells with indications of relevant parameters for calculating 2D pair distributions. This figure is a modification of the one reported in ref 23.
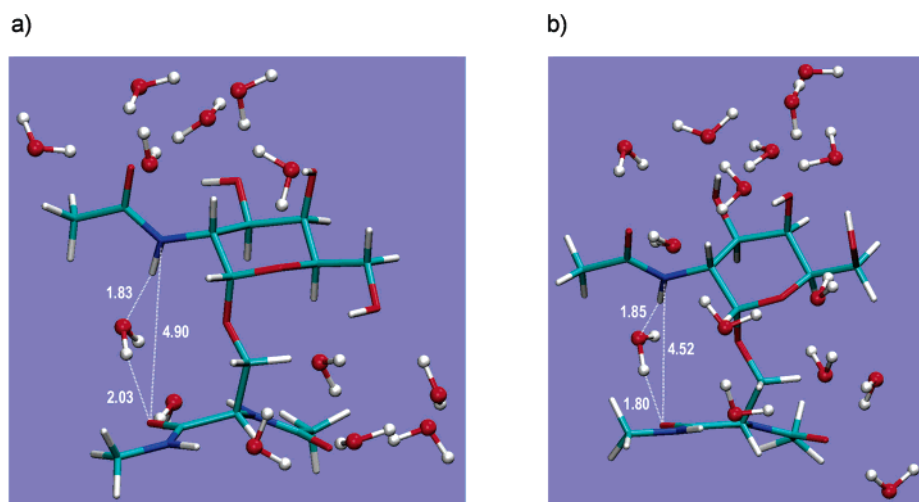
$$g(r_1, r_2) = \frac{N(r_1, r_2)}{\rho_w \cdot V_i(r_1, r_2, \Delta r)}$$

$N(r_1, r_2)$ = *probability*
ρ_ω = *water density*
V_i = *volume of intersection*

Figure 5. Calculated B3LYP/6-31G(d) geometries of compound **1**, including the surrounding water molecules from two different frames of the MD$_{H2O}$-tar trajectory: (a) gauche (−) conformation for the hydroxymethyl group and (b) gauche (+) conformation for the same group.

inclusion of explicit water molecules that solvate the polar groups of **1** is crucial to obtain a structure according to that experimentally observed. The obtained results suggest that not only the bridging water molecule but also the surrounding water molecules are important for stabilization of the extended conformation of the backbone. Indeed, the systematic removal of some crucial solvent molecules produced severe alterations on the solute structure, especially on the backbone conformation.

For example, if only the bridging water molecule is removed, the backbone preserves the extended conformation and the hydrogen bond between H3 and O1 is not observed. On the other hand, if all the water molecules are removed except the one involved in the water bridge, the obtained geometry cannot accurately reproduce the experimental data. Some of these geometries are displayed in the Supporting Information, for illustrative purposes. As a consequence, the geometry calculated

in vacuo for the same compound by Csonka et al. at the HF/6-31G(d) level[1c] considerably differs from that proposed in this paper, as shown in Figure 3a (see the red square). The reported calculations carried out in vacuo predict a γ_L-turn conformation for the backbone, stabilized by two key hydrogen bonds, one between O2⋯H1 and another one between O1⋯H3. On the contrary, our structure is similar to that proposed by Danishefsky and co-workers for the tri-α-STF−STTAV glycopeptide,[1b] a short mucin motif of glycoprotein CD43 (Figure 3a, yellow circle). For this more complex glycopeptide, the experimental distance N3⋯O1 was experimentally measured to fluctuate from 3.2 to 4.1 Å (in compound **1**, as commented above, this distance between these two atoms ranged from 2.8 to 7.8 Å) with the corresponding angle N3−H3−O1 being close to 96° (the average angle obtained for **1** from the MD-tar simulations was 120 ± 22°). Taking into account these experimental values, the authors indicated that it is difficult to certainly assert whether the peptide−sugar interactions are more appropriately viewed as electrostatic or should be seen as conventional hydrogen bonds. In this paper, we propose a completely different point of view, perfectly compatible with the experimental data, and in which, as commented above, water molecules play a crucial role.

Conclusions. In contrast to common belief, the structural study of the mucin-type simplest model glycopeptide, α-*O*-GalNAc-L-Ser diamide, reveals that intramolecular hydrogen bonds involving sugar and peptide residues are very weak, and consequently, they cannot determine the defined geometry of this type of molecule. Our experimental and theoretical results point toward the existence of water pockets/bridges between the sugar and the peptide moieties and indicate that the surrounding water molecules are essential to keep the defined conformation. Although these results are on the smallest model glycopeptide, the existence of such sugar−peptide interactions through bridging water molecules could explain the particular features of mucin-type glycoproteins. The combined experimental/theoretical investigations of synthetically prepared larger systems are currently underway.

Experimental Section

General Procedures. Solvents were purified according to standard procedures. Analytical TLC was performed using Polychrom SI F254 plates. Column chromatography was performed using silica gel 60 (230−400 mesh). ^{1}H and ^{13}C NMR spectra were recorded on Bruker ARX 300, Bruker Avance 400, and Bruker Avance 500 spectrometers. ^{1}H and ^{13}C NMR spectra were recorded in CDCl$_3$ and CD$_3$OD with TMS as the internal standard and in D$_2$O (chemical shifts are reported in ppm on the δ scale). Melting points were determined on a Büchi B-545 melting point apparatus and are uncorrected. Optical rotations were measured on a Perkin-Elmer 341 polarimeter. Microanalyses were carried out on a CE Instruments EA-1110 analyzer and are in good agreement with the calculated values.

Synthesis of Compound 2. A solution of ^{13}C-labeled (*S*)-serine (1.04 g, 9.8 mmol) in 1 N aqueous NaOH (20 mL) and dioxane (10 mL) at 0 °C was treated with di-*tert*-butyl dicarbonate (2.57 g, 11.8 mmol) and the mixture was allowed to warm to room temperature and stirred for 24 h. The dioxane was then evaporated and the aqueous layer was washed with Et$_2$O (30 mL) to remove di-*tert*-butyl dicarbonate. Ethyl acetate (50 mL) was then added to the aqueous layer and the mixture stirred while a 1 M aqueous H$_2$SO$_4$ solution was added to give pH 2−3. Following the separation of the organic layer, the aqueous layer was then saturated with NaCl and extracted with ethyl acetate (4 × 50

mL). The combined organic layers were dried and filtered and the solvent was removed to give quantitatively ^{13}C-labeled *N*-Boc-(*S*)-serine as a thick oil (2.02 g). A solution of this compound (500 mg, 2.43 mmol) in acetonitrile (60 mL) was treated with diisopropilethylamine (DIEA) (2.0 mL, 12.1 mmol), methylamine hydrochloride (328 mg, 4.85 mmol), and *O*-benzotriazol-1-yl-1,1,3,3-tetramethyluronium tetrafluoroborate (TBTU) (935 mg, 2.91 mmol) under an inert atmosphere. The reaction mixture was stirred at room temperature for 10 h, the solvent was then removed, and the mixture was partitioned between brine (20 mL) and ethyl acetate (70 mL). The organic layer was washed with 0.1N HCl (2 × 20 mL) and 5% NaHCO$_3$ (2 × 20 mL), dried over anhydrous Na$_2$SO$_4$, filtered, and evaporated to give a residue that was purified by silica gel column chromatography, eluting with dichloromethane/MeOH (94:6) to give **2** (341 mg), as a white solid, in 64% yield. Mp 122−124 °C. [α]$^{25}_D$ = −20.8 (*c* 1.55, CHCl$_3$). ^{1}H NMR (400 MHz, CDCl$_3$): δ 1.44 (s, 9H), 2.82 ('t', *J* = 4.0 Hz, 3H), 3.56−3.77 (m, 1H), 4.02−4.11 (m, 1H), 4.11−4.19 (m, 1H), 5.59−5.69 (m, 1H), 6.70−6.84 (m, 1H). ^{13}C NMR (100 MHz, CDCl$_3$): δ 26.2, 28.3, 55.0, 63.0, 80.6, 156.3, 172.0. Anal. Calcd for C$_8$^{13}CH$_{18}$N$_2$O$_4$: C, 49.76; H, 8.28; N, 12.78. Found: C, 49.58; H, 8.26; N, 12.76.

Synthesis of Compound 3. TFA (5 mL) was added to a solution of **2** (300 mg, 1.37 mmol) in CH$_2$Cl$_2$ (5 mL) at 0 °C. The reaction was maintained at 0 °C for 30 min and at room temperature for 3 h and then concentrated. The residue was then dissolved in pyridine/acetic anhydride (3:1, 8 mL) and stirred at room temperature for 3 h to give the corresponding diacetylated compound, which was used in the next step without purification. This compound was then dissolved in MeOH (5 mL) and treated with sodium methoxide/MeOH (0.5 M) to pH 9. After stirring at room temperature for 3 h, the mixture was neutralized with Dowex 50-X8, filtered, and concentrated. Finally, the residue was purified by silica gel column chromatography, eluting with dichloromethane/methanol (85:15) to give **3** (161 mg), as a white solid, in 73% yield. Physical properties were identical to those reported in the literature.[11] Anal. Calcd for C$_5$^{13}CH$_{12}$N$_2$O$_3$: C, 45.33; H, 7.50; N, 17.38. Found: C, 45.22; H, 7.51; N, 17.35. ^{1}H NMR (400 MHz, D$_2$O): δ 2.08 (s, 3H), 2.77 (s, 3H), 3.80−3.91 (m, 2H), 4.36−4.40 (m, 1H). ^{13}C NMR (100 MHz, D$_2$O): δ 22.7, 26.4, 57.0, 63.0, 173.1, 173.5.

Synthesis of Compound 4. Concentrated HNO$_3$ (10% ^{15}N-labeled) (1 mL) was added dropwise to acetic anhydride (10 mL) at 10 °C under constant stirring. The external temperature was further lowered to −10 °C to keep the internal temperature in the range 10−20 °C during the addition. Once the addition was completed, the solution was cooled further to −50 °C upon which a precipitate formed. Then a solution of tri-(*O*-benzyl)galactal (1.00 g, 2.4 mmol) in acetic anhydride (5 mL) was added over a period of 10−15 min, and the mixture stirred at this temperature for 30 min. After the reaction mixture had been allowed to warm to −22 °C, it became clear. The reaction mixture was then poured into cold water (20 mL), brine (10 mL) was added, and the aqueous layer was extracted with Et$_2$O (3 × 10 mL). The combined organic layers were dried (Na$_2$SO$_4$) and the solvents removed by coevaporation with toluene. The corresponding crude 2-nitrogalactopyranose derivative was dissolved in dichloromethane (10 mL) and slowly added to an ice-cold, stirred solution of triethylamine (0.36 mL, 2.60 mmol) in dichloromethane (5 mL). After complete addition, the cooling bath was removed and stirring was continued for 30 min, at room temperature. The organic phase was washed with 2 N HCl solution and dried (Na$_2$SO$_4$). Removal of the volatiles and silica gel column chromatographic purification (toluene/ethyl acetate, 98:2) of the residue gave compound **4** (897 mg), as a light yellow oil, in 81% yield. Physical properties and spectral data were identical to those reported in the literature.[8] Anal. Calcd for C$_{27}$H$_{27}$NO$_6$: C, 70.25; H, 5.91; N, 3.06. Found: C, 70.11; H, 5.92; N, 3.01.

Synthesis of Compounds 5α and 5β. Compounds **3** (97 mg, 0.61 mmol) and **4** (234 mg, 0.51 mmol) were dissolved in THF (5 mL) under argon, and freshly activated molecular sieve (3 Å, 0.5 g) was then added. After stirring of the reaction mixture at room temperature

for 1 h, 1 M potassium *tert*-butoxide solution in THF (51 μL, 0.05 mmol) was added and stirring was continued for 12 h. Acetic acid (2 mL) was used to acidify the reaction mixture, the molecular sieve was filtered off, and all solvents were removed by evaporation. The residue was purified by silica gel column chromatography (ethyl acetate/methanol, 95:5) to give a mixture of **5α** and **5β** in a 9:1 ratio (190 mg), as an oil, in 60% yield. Optical rotation for this mixture: $[\alpha]^{25}_D = +31.0$ ($c = 0.61$, CH$_3$OH). Compound **5α**: ^{1}H NMR (400 MHz, CDCl$_3$): δ 2.00 (s, 3H), 2.76 (d, $J = 4.8$ Hz, 3H), 3.48−3.61 (m, 2H), 3.65 (dd, $J = 10.9$ Hz, $J = 6.6$ Hz, 1H), 3.94 (dd, $J = 10.9$ Hz, $J = 5.2$ Hz, 1H), 3.97−4.00 (m, 2H), 4.36 (dd, $J = 10.6$ Hz, $J = 2.8$ Hz, 1H), 4.40−4.51 (m, 4H), 4.66−4.74 (m, 2H), 4.83 (d, $J = 11.2$ Hz, 1H), 5.02 (dd, $J = 10.6$ Hz, $J = 4.8$ Hz, 1H), 5.40 (d, $J = 4.2$ Hz, 1H), 6.08−6.14 (m, 1H), 6.38 (d, $J = 7.5$ Hz, 1H) 7.20−7.38 (m, 15H). ^{13}C NMR (100 MHz, CDCl$_3$): δ 23.1, 26.4, 52.5, 68.2, 68.6, 70.2, 72.7, 72.9, 73.7, 74.9, 75.0, 84.4, 96.9, 128.0, 128.1, 128.2, 128.2, 128.2, 128.4, 128.5, 128.6, 137.0, 137.4, 137.7, 169.5, 170.2.

Synthesis of Compound 6α. Platinized Raney nickel (T4) catalyst was freshly prepared as described in ref. 10. The catalyst obtained using 2 g of Raney nickel/aluminum alloy was suspended in ethanol (10 mL) and prehydrogenated for 10 min before the addition of the mixture of glycosides **5α** and **5β** (180 mg, 0.29 mmol) in ethanol (7 mL). The reaction mixture was shaken under H$_2$ (1 atm) for 3 h at room temperature. The catalyst was filtered off and the solvent evaporated. The residue was dissolved in pyridine/acetic anhydride (2:1, 6 mL) and stirred at room temperature for 3 h. Removal of the volatiles and silica gel column chromatographic purification (ethyl acetate/methanol, 95:5) gave an oil corresponding to α-glycoside **6α** (153 mg) in 83% yield. $[\alpha]^{25}_D = +28.1$ ($c = 0.4$, MeOH). ^{1}H NMR (400 MHz, CD$_3$-OD-CDCl$_3$): δ 1.93 (s, 3H), 1.97 (s, 3H), 2.63−2.67 (m, 3H), 3.41 (dd, $J = 9.7$ Hz, $J = 4.2$ Hz, 1H), 3.58−3.71 (m, 3H), 3.88−3.94 (m, 2H), 4.20 (dd, $J = 11.4$ Hz, $J = 2.6$ Hz, 1H), 4.38−4.75 (m, 7H), 4.90 (d, $J = 3.6$ Hz, 1H), 4.95 (d, $J = 11.7$ Hz, 1H), 5.55 (d, $J = 8.5$ Hz, 1H), 6.36−6.42 (m, 1H), 7.07 (d, $J = 8.6$ Hz, 1H), 7.26−7.40 (m, 15H). ^{13}C NMR (100 MHz, CD$_3$OD-CDCl$_3$): δ 20.7, 21.0, 24.5, 48.5, 52.8, 67.3, 67.3, 68.3, 69.2, 71.0, 72.5, 73.7, 76.5, 98.0, 126.4, 126.6, 126.6, 126.7, 126.8, 127.0, 127.1, 127.3, 127.4, 137.1, 137.6, 137.7, 169.5, 170.3, 171.2. Anal. Calcd for C$_{34}$^{13}CH$_{43}$N$_3$O$_8$: C, 66.37; H, 6.84; N, 6.63. Found: C, 66.52; H, 6.77; N, 6.59.

Synthesis of Compound 1. To a solution of glycoside **6α** (14 mg, 0.02 mmol) in ethyl acetate/methanol (1:1) (3 mL) was added 10% palladium−carbon (7 mg) as a catalyst. The reaction mixture was shaken under H$_2$ (1 atm) for 12 h at room temperature. Removal of the catalyst and the solvent gave **1** (8 mg), as a colorless oil, in quantitative yield. Data for ^{13}C- and ^{15}N-labeled compound **1**: $[\alpha]^{25}_D = +24.1$ ($c = 0.54$, CH$_3$OH). ^{1}H NMR (400 MHz, D$_2$O): δ 2.04 (s, 3H), 2.07 (s, 3H), 2.70−2.78 (m, 3H), 3.71−3.77 (m, 2H), 3.78−3.85 (m, 1H), 3.85−3.95 (m, 3H), 3.96−4.01 (m, 1H), 4.14 (dd, $J = 11.0$ Hz, $J = 3.7$ Hz, 1H), 4.50−4.57 (m, 1H), 4.89 (d, $J = 3.5$ Hz, 1H). ^{13}C NMR (100 MHz, D$_2$O): δ 21.8, 22.0, 26.0, 49.8, 54.2, 61.2, 67.1, 67.6, 68.4, 71.3, 97.8, 171.3, 171.9, 174.4. Anal. Calcd for C$_{13}$^{13}CH$_{25}$N$_3$O$_8$: C, 46.41; H, 6.93; N, 11.56. Found: C, 46.54; H, 7.05; N, 11.41. Data for compound **1** at natural abundance: $[\alpha]^{25}_D = +24.8$ ($c = 0.51$, CH$_3$-OH). ^{1}H NMR (400 MHz, D$_2$O): δ 2.05 (s, 3H), 2.08 (s, 3H), 2.76 (s, 3H), 3.72−3.78 (m, 2H), 3.81 (dd, $J = 10.8$ Hz, $J = 5.5$ Hz, 1H), 3.86−3.94 (m, 3H), 3.97−4.00 (m, 1H), 4.15 (dd, $J = 11.0$ Hz, $J = 3.7$ Hz, 1H), 4.54 (dd, $J = 5.5$ Hz, $J = 4.5$ Hz, 1H), 4.89 (d, $J = 3.7$ Hz, 1H). ^{1}H NMR (500 MHz, H$_2$O/D$_2$O): δ 2.05 (s, 3H), 2.08 (s, 3H), 2.76 (d, $J = 4.6$ Hz, 3H), 3.72−3.78 (m, 2H), 3.81 (dd, $J = 10.8$ Hz, $J = 5.5$ Hz, 1H), 3.86−3.94 (m, 3H), 3.97−4.00 (m, 1H), 4.15 (dd, $J = 11.0$ Hz, $J = 3.7$ Hz, 1H), 4.54 (m, 1H), 4.89 (d, $J = 3.7$ Hz, 1H), 8.05 (d, $J = 9.2$ Hz, 1H), 8.05−8.12 (m, 1H), 8.42 (d, $J = 6.2$ Hz, 1H). Anal. Calcd for C$_{14}$H$_{25}$N$_3$O$_8$: C, 46.28; H, 6.93; N, 11.56. Found: C, 46.39; H, 7.00; N, 11.40.

2D NMR Experiments. NMR experiments were recorded on a Bruker Avance 400 spectrometer at 293 K. Magnitude-mode ge-2D COSY spectra were recorded with gradients and using the cosygpqf pulse program with 90° pulse width. Phase-sensitive ge-2D HSQC spectra were recorded using *z*-filter and selection before t_1 removing the decoupling during acquisition by use of the invigpndph pulse program with CNST2 (JHC) = 145. 2D NOESY experiments were made using phase-sensitive ge-2D NOESY for CDCl$_3$ spectra and phase-sensitive ge-2D NOESY with WATERGATE for H$_2$O/D$_2$O (9: 1) spectra. Selective ge-1D NOESY experiments were carried out using the 1D-DPFGE NOE pulse sequence. NOEs intensities were normalized with respect to the diagonal peak at zero mixing time. Experimental NOEs were fitted to a double exponential function, $f(t) = p_0[\exp(-p_1t)][1 - \exp(-p_2t)]$ with p_0, p_1, and p_2 being adjustable parameters.[13] The initial slope was determined from the first derivative at time $t = 0$, $f'(0) = p_0p_2$. From the initial slopes, interproton distances were obtained by employing the isolated spin pair approximation.

Experimental Determination of $J_{C,H}$ Coupling Constants. 1D-Selective HMQC-type experiments[21b] were performed on the ^{13}C-labeled samples on a Bruker AVANCE 500 at 278 K. The ^{13}C hard 90° pulses in the regular HMQC sequence were replaced by soft Gaussian-shape pulses of 40 ms length and centered on the carbonyl resonance frequency. Different experiments were performed with the period for evolution of couplings (1/2*J*) chosen to match *J* values of 1, 2, 3, 4, and 5 Hz (See Supporting Information). No refocusing period was used and the resulting 1H spectra were processed both in the phase-sensitize and magnitude modes. A total of 1024 scans were acquired per experiment with a repetition delay of 4 s and an acquisition time of 1.5 s

Computational Methods. Molecular Dynamics Simulations: MD-tar Simulations. NOE-derived distances (see Table 2) were included as time-averaged distance constraints and scalar coupling constants *J* as time-averaged coupling constraints. A $\langle r^{-6}\rangle^{-1/6}$ average was used for the distances and a linear average was used for the coupling constants. Final trajectories were run using an exponential decay constant of 8000 ps and a simulation length of 80 ns for the MD-tar simulation with $\epsilon = 80$ and using an exponential decay constant of 400 ps and a simulation length of 4 ns for the MD-tar simulations in explicit water (MD$_{H_2O}$-tar).

Molecular Modeling in Explicit Water. The solute molecule was first immersed in TIP3P[24] bath water molecules with the LEAP module.[25] The simulation was performed using periodic boundary conditions and the particle-mesh Ewald approach[26] to introduce long-range electrostatic effects. The SHAKE algorithm[27] for hydrogen atoms, which allows using a 2-fs time step, was also employed. Finally, a 9-Å cutoff was applied to Lennard-Jones interactions. Equilibration of the system was carried out as follows; as a first step, a short minimization with positional restraints on solute by a harmonic potential with a force constant of 500 kcal mol^{-1} Å^{-2} was done. A 12.5-ps molecular dynamics calculation at 300 K maintaining positional restraints on the solute was then run in order to equilibrate the water box. For these two steps, a 9-Å cutoff was used for the treatment of the electrostatic interactions. As the next step, the system was equilibrated during an additional 12.5-ps period, but using now the mesh Ewald method, as water properties are slightly different with this treatment. Then, the system was subjected to several minimization cycles, gradually reducing positional restraints on the solute from 500 to 0 kcal mol^{-1} Å^{-2}. Finally, one unrestrained MD trajectory at constant pressure (1 atm) and temperature (300 K) was collected and analyzed using the CARNAL module.[28] The simulation length was 40 ns.

(24) Chiansan, M.; Baner, N. A.; Simpson, J.; McCammon, J. A. *J. Am. Chem. Soc.* **2002**, *124*, 1438−1442.
(25) Schafmeister, C. E. A. F.; Ross, W. F.; Romanovsky, V. University of California, San Francisco, 1995.
(26) Darden, C. S. A. T. *Annu. Rev. Biophys. Biomol. Struct.* **1999**, *28*, 155−179.
(27) Rykaert, J. P.; Ciccote, G.; Berendsen, J. C. *J. Comput. Phys.* **1977**, *23*, 327−341.
(28) Ross, W. S. Carnal: Coordinate Analysis Program 1999, Department of Pharmaceutical Chemistry, University of California, San Francisco.

DFT Calculations. All calculations were carried out by means of the B3LYP hybrid functional.[29] Full geometry optimizations were carried out with the 6-31G(d) basis set using the Gaussian 03 package.[30] BSSE corrections were not considered in this work. Analytical frequencies were calculated at the same level to determine the nature of the optimized geometries. Scaled frequencies were not considered because significant errors on the calculated thermodynamical properties are not found at his theoretical level. Solvent effects were included in geometry optimizations using explicit water molecules from the first hydration shell.

Supporting Information Available: ^{1}H and ^{13}C NMR spectra of compounds **1**, **2**, **3**, **5α**, and **6α**, as well as COSY and HSQC correlations of compound **1**, **5α**, and **6α**; MD simulations in explicit water for derivative **1** and B3LYP/6-31G(d) distances, dihedral angles, energy, enthalpy, free energy, entropy, and coordinates of the optimized structures of **1** together with explicit water molecules; 1D-selective HMQC-type experiments; MPEG movie of the MD-tar trajectory (5 ps) in explicit water showing one bridging water molecule; and complete refs 16b and 30. This material is available free of charge via the Internet at http://pubs.acs.org.

JA064539U

(29) (a) Lee, C.; Yang, W.; Parr, R. *Phys. Rev. B* **1988**, *37*, 785−789. (b) Becke, A. D. *J. Chem. Phys.* **1993**, *98*, 5648−5652.
(30) Pople, J. A.; et al. Gaussian 03, Revision C.01; Gaussian, Inc.: Wallingford, CT, 2004.